www.czasopisma.pan.pl PAN POLSKA AKADEMIA NAUK www.journals.pan.pl

THE ARCHIVE OF MECHANICAL ENGINEERING

VOL. LVIII 2011 Number 1

10.2478/v10180-011-0006-6

Key words: inspection, pipeline, mobile robot, design, prototype

ADRIAN ALUŢEI[*], *MIHAI OLIMPIU TĂTAR*[*], *VISTRIAN MĂTIEŞ*[*]

THE DEVELOPMENT OF A MODULAR INSPECTION SYSTEM

The aim of this paper is to present an in-pipe modular robotic system that can navigate inaccessible industrial pipes in order to check their condition, locate leakages, and clean the ventilation systems. The aspects concerning the development of a lightweight and energy efficient modular robotic system are presented. The paper starts with a short introduction about modular inspection systems in the first chapter, followed by design aspects and finalizing with the test of the developed robotic system.

1. Introduction

In the mining, gas and petroleum industries, maintenance and inspection represents is a problem of great concern. Accidents and high-priced full pipeline replacements can be avoided by the use of a robotic in-pipe inspection system that can give visual and sensorial data about the status of portions of the pipeline [1], [2], [3]. Taking in consideration the inaccessible workspace, the structure of the robotic system must be modular and most important adaptable. The most solicitant position in which the robot has to work is represented by vertical and elbow pipe portions. The control of the modular robotic system is done from a distance. The main advantages of these modular systems are versatility, simple design, lightweight robust modules, low energy consumption and low cost of fabrication.

2. Design of the modular robotic system

The configuration of the modules of the robot system is presented in Figure 1:

[*] *Technical University of Cluj-Napoca, Department Mechanisms, Precision Mechanics and Mechatronics, Romania; e-mail: alutei.adrian@gmail.com, olimpiut@yahoo.com, matiesvistrian@yahoo.com.*

www.czasopisma.pan.pl PAN POLSKA AKADEMIA NAUK www.journals.pan.pl

Fig. 1. Configuration of the robotic system

2.1. The active module design

The presented active module is composed of 3 slider-crank mechanisms placed at 120° angles around the central axle. This structure can adapt more easily to the variation of the pipe's diameter. The wheels of the active module are pressed against the inner surface of the inspected pipe using two compression springs placed one on each side of the module's central axle [4]. [5].

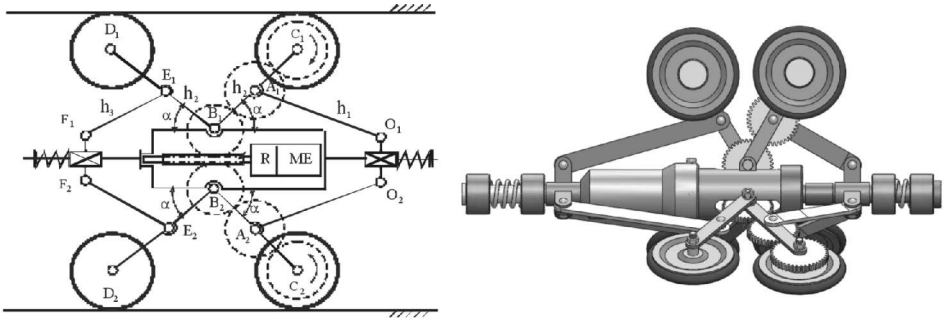

Fig. 2. Active module design

Based on the structural scheme from figure 2, the variation of the adaptable mechanism will provide the maximum and minimum diameter of the inspected pipes as follows:

$$H = 2R + 2a + 2h_2 \sin\alpha \tag{1}$$

where R represents the active wheel radius, $H = D$ the pipe diameter, and α=*15-60*^{0}. Thus, the robot can inspect pipes with diameter values between *Ø130 - Ø170*.

The specially designed wheels have a radius of r = 25 mm, a length of 7 mm and the component elements have the lengths: *h1 = 95 mm, h2 = 58 mm, h3= 53 mm.* The actuator is positioned in the centre of the active module and the transmission is done trough a worm-gear mechanism. The transmission system is composed of the following elements:

- 1 – single-enveloping worm ($z_1 = 1$, module $m = 0,75$ mm, angle of the worm spiral $\theta = 4^0$),
- 2, 3, 4 – gears with angled teeth (teeth angle is $\beta = 4^0$)
- $z_2 = 42$, $z_3 = 38$, $z_4 = 38$ – number of teeth.

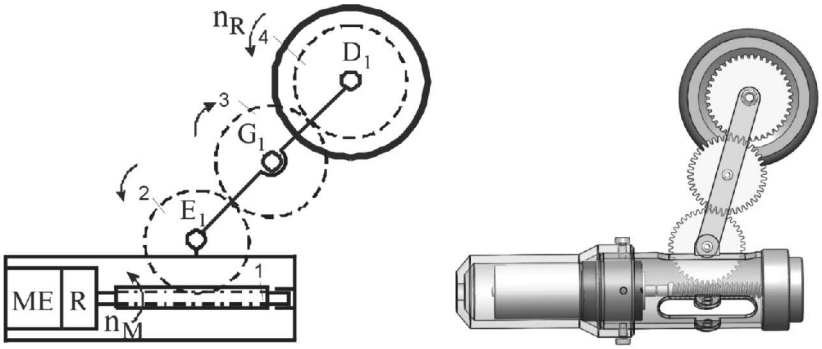

Fig. 3. Transmission of movement for the active module

The worm-gear mechanism transmits the movement from the axle of the motor reducing rotational speed. A high value of motor torque is then necessary. The transmission ratio is:

$$i_{transmisie} = \frac{n_M}{n_R} = i_{12} \cdot i_{23} \cdot i_{34} = \frac{z_4}{z_1} = 38 : 1 \tag{2}$$

The assembly between the gear wheel and the active wheel of the designed robot is made using a specially designed shaft. The gear wheel is mounted on the axle trough a wedge and the active wheel is serried mount as presented in Figure 4.

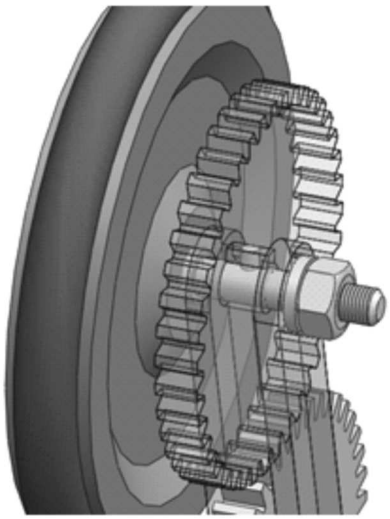

Fig. 4. Gearwheel assembly

The material used for the active module is mostly aluminum, a soft and lightweight metal. The designed length of the active module is *307 mm* and the expected weight is *0,590 kg*.

www.czasopisma.pan.pl PAN POLSKA AKADEMIA NAUK www.journals.pan.pl

2.2. The passive module design

Two types of passive modules are proposed. The first passive module has the task of transporting the electronic equipment and the batteries that power the actuators. It has a cylindrical shape and six wheels, three at each end of the module, placed at 120° angles around the longitudinal axis. The axle of each individual wheel is mounted in a fork-like clamping system which is placed on a rod with a compression spring that allows the wheel to slide along an axis that is perpendicular on the longitudinal axis of the module. In this way the module can cross sections of pipe with different diameters. The 3D model of the passive module is presented in Figure 5.

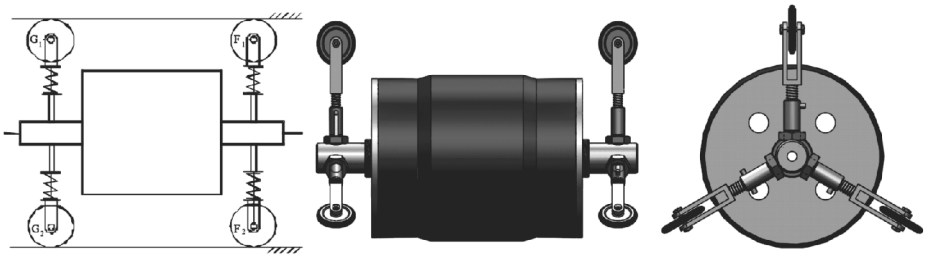

Fig. 5. First passive module design

The second passive designed module could be used for the transport of electronic or energy accumulators. The wheels of the passive module have the radius $r = 25$ [mm], width of 7 [mm] and the kinematic elements have the lenghts: $h_1 = 30$ [mm], $h_2 = 70$ [mm], $h_3 = 135$ [mm], ($h_1 = O'_1A_1 = O'_2A_2 = O'_3A_3, h_2 = E'_1D_1 = E'_2D_2 = E'_3D_3,, h_3 = C'_1F_1 = C'_2F_2 = C'_3F_3$). In Figure 6 the second passive module design is presented.

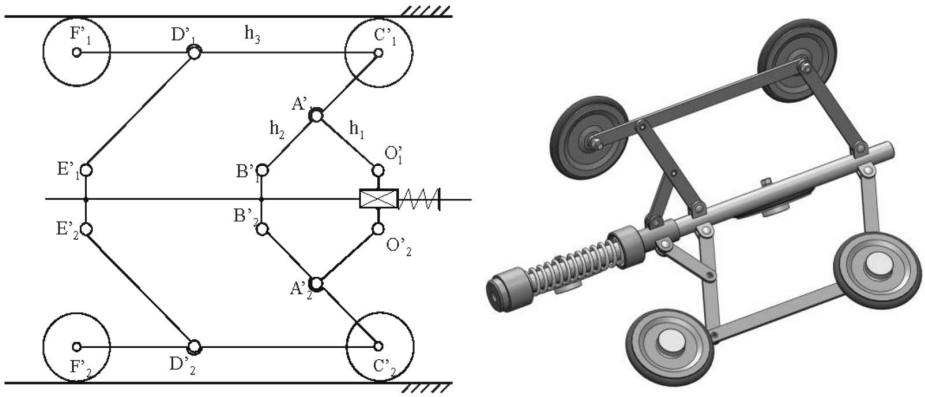

Fig. 6. Second passive module design

2.3. Auxiliary modules design

Auxiliary modules are represented by the protection case for the wireless video-camera and the universal joint that connects the modules. In Figure 7 the 3D, the designed video-camera protection case and the universal joint are presented.

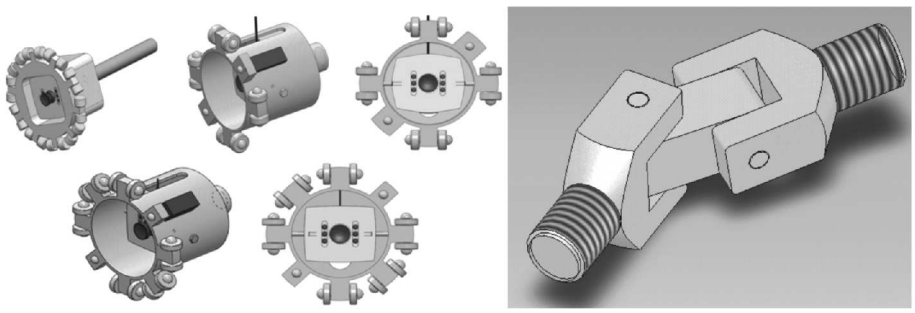

Fig. 7. Auxiliary modules design

The universal joint mechanical resistance was tested for the extreme case of displacement in a vertical pipe segment using FEM analysis with CosmosXpress add-on from SolidWorks. The value of the maximum force at which the universal joint must be resistant is:

$$G_T = M_T \cdot g = 2,085 \cdot 9,8 = 20,433[N] \tag{3}$$

The adopted material for the universal joint was OL60 and the following results are presented in Figure 8.

The maximum yield stress value is $2,41\ x\ 10^8 N/m^2$, as can be seen in figure 8a, and in the FEM analisys the distribution also with the maximum strenght for the piece is $1,675\ x\ 10^6\ N/m^2$. The piece resists and the maximum displacement that apears in the piece is $6,698\ x\ 10^{-5}\ mm$. In Figure 8c, the maximum value for the stress in the piece is $2.089\ x\ 10^6\ N/m^2$ and the yield strenght of the material is $6,204\ x\ 10^8\ N/m^2$.

2.4. Mathematic model of the robot

We take into consideration the case in which the system is traveling upwards in a vertical pipe segment. For developing the mathematical model, the following annotation were made: $\bar{F}_f$ as the friction force between the wheel and the pipe wall, $F_f = \mu \cdot F_R$, where $\bar{F}_R$ is the reaction force between the wheel and the pipe wall; $\bar{M}_{fr}$ as the rolling friction torque $M_{fr} = s \cdot F_R$, where s is the rolling friction coefficient; μ as the slip friction coefficient, $\bar{\omega}_R$ as the angular speed of the wheel, d as the diameter of the wheel axle,

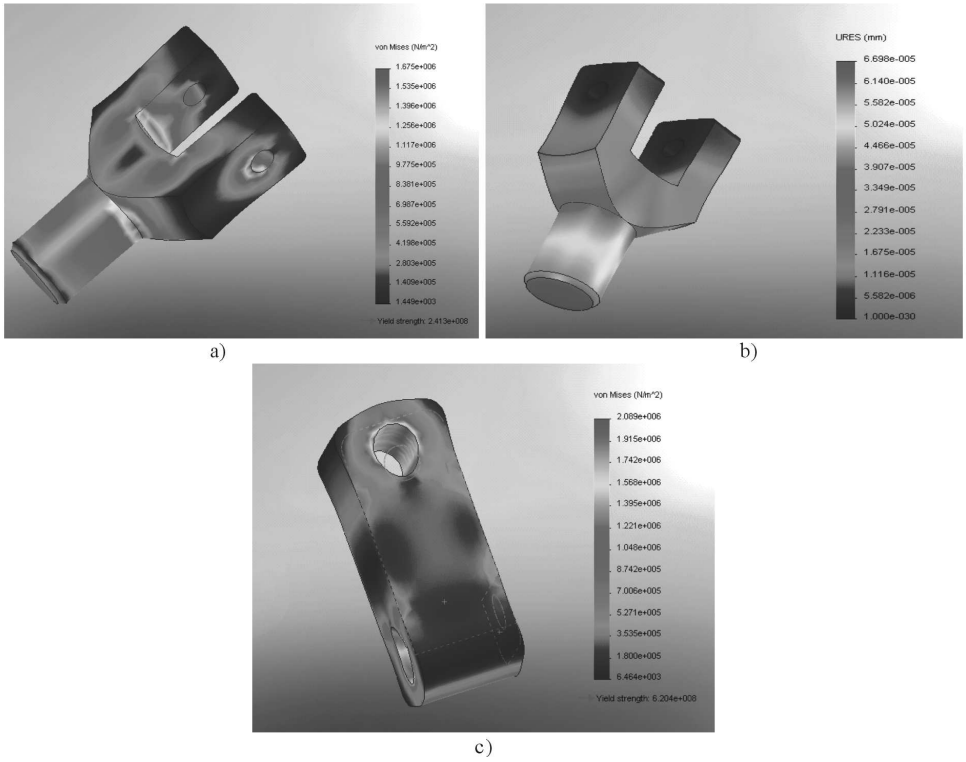

Fig. 8. FEM analysis with CosmosXpress for the universal joint in the most solicitant case

k as the active module's springs constant, R as the wheel's radius, v as the robot's speed $v = \omega_R R$,G as the weight force of the active module, m_1 as the actual mass of the active module, $\bar{M}^r_{r\,axRM}$ represents the resistant reduced torque of the actuator's axle, $\overline{M}_{fl}$ represents the friction torque in the wheel bearing and has the expression:

$$M_{fl} = \frac{\mu \cdot d \cdot F_R}{2} \tag{4}$$

The force distribution along the robotic arm of the active module is presented in Figure 9.

Based on the mechanism from Figure 9, the following equations are used for each of the two active kinematic elements in the active module:

$$F_{R1} = F_{A1} \cdot tg\alpha = k\Delta x_1 \cdot tg\alpha \tag{5}$$

$$F_{R2} = F_{A2} \cdot tg\alpha = k\Delta x_2 \cdot tg\alpha \tag{6}$$

The equations of variation of the two spring's displacement Δx_1 and Δx_2 are:

www.czasopisma.pan.pl PAN POLSKA AKADEMIA NAUK www.journals.pan.pl

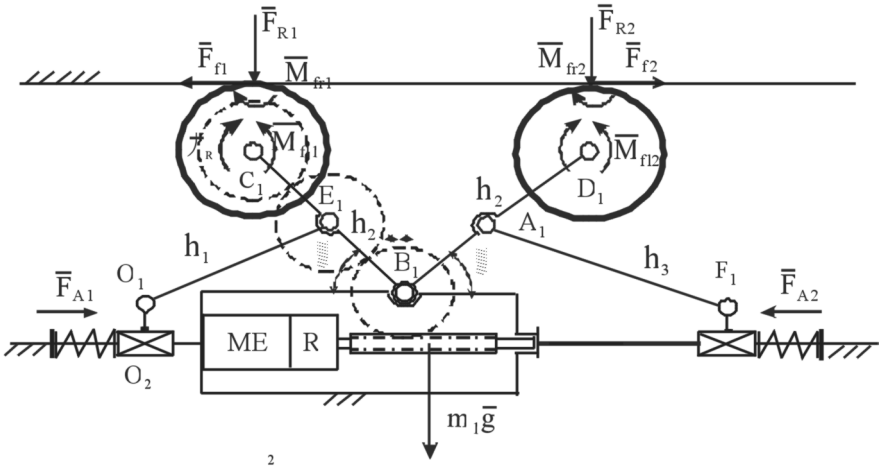

Fig. 9. Force distribution in the active module

$$\Delta x_1 = h_2(\cos\alpha_{\max} - \cos\alpha) + \\ + \sqrt{h_2^2\cos\alpha - 4[(e_2-e_1)^2 + \frac{h_2^2}{4} + (e_2-e_1)h_2\sin\alpha_{\max} - h_1^2]} - \\ - \sqrt{h_2^2\cos\alpha - 4[(e_2-e_1)^2 + \frac{h_2^2}{4} + (e_2-e_1)h_2\sin\alpha - h_1^2]} \tag{7}$$

$$\Delta x_2 = h_2(\cos\alpha_{\max} - \cos\alpha) + \\ + \sqrt{h_2^2\cos\alpha - 4[(e_2-e_1)^2 + \frac{h_2^2}{4} + (e_2-e_1)h_2\sin\alpha_{\max} - h_3^2]} - \\ - \sqrt{h_2^2\cos\alpha - 4[(e_2-e_1)^2 + \frac{h_2^2}{4} + (e_2-e_1)h_2\sin\alpha - h_3^2]} \tag{8}$$

The equation of the reduced torque at the actuator's axle, taking in consideration the whole system, will be:

$$M^r_{raxM} = \frac{1}{i_{reductor}i_{transmisie}} \\ \left[3\left(M_{fr1} + M_{fl1}\right) + 3\left(M_{fr2} + M_{fl2}\right) + v\cdot G_1 + \frac{1}{2}\left[6\left(M_{frp} + M_{flp}\right) + vG_2\right]\right] \tag{9}$$

www.czasopisma.pan.pl PAN POLSKA AKADEMIA NAUK www.journals.pan.pl

Transformed in:

$$M^r_{raxM} = \frac{1}{i_{reductor} i_{transmisie}} \left[3F_{R1}\left(s + \frac{\mu d}{2}\right) + Rm_1 g + 3F_{R2}\left(s + \frac{\mu d}{2}\right) + \frac{1}{2}R_p m_2 g + 3k_2 \Delta x\left(s + \frac{\mu d}{2}\right)\right] \tag{10}$$

The variation of the reduced torque at the axle of the actuator is presented in Figure 10.

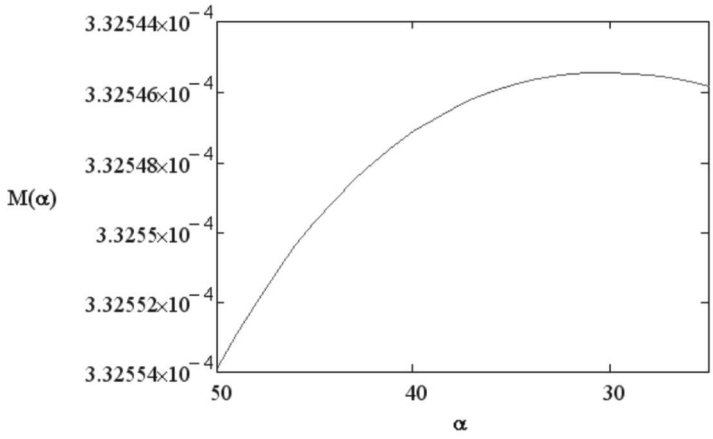

Fig. 10. The variation of the resistant torque reduced at the axle of the motor in respect with α angle

The maximum value calculated for the reduced torque at the axle of the actuator, considered for the simulation of the whole system is of $3.510^{-4} Nm$.

2.5. The model and simulation results for the robot

The DC motor and the transmission model were made using Matlab/ Simulink and is presented in Figure 11:

The results of the simulation are presented in Figure 12:

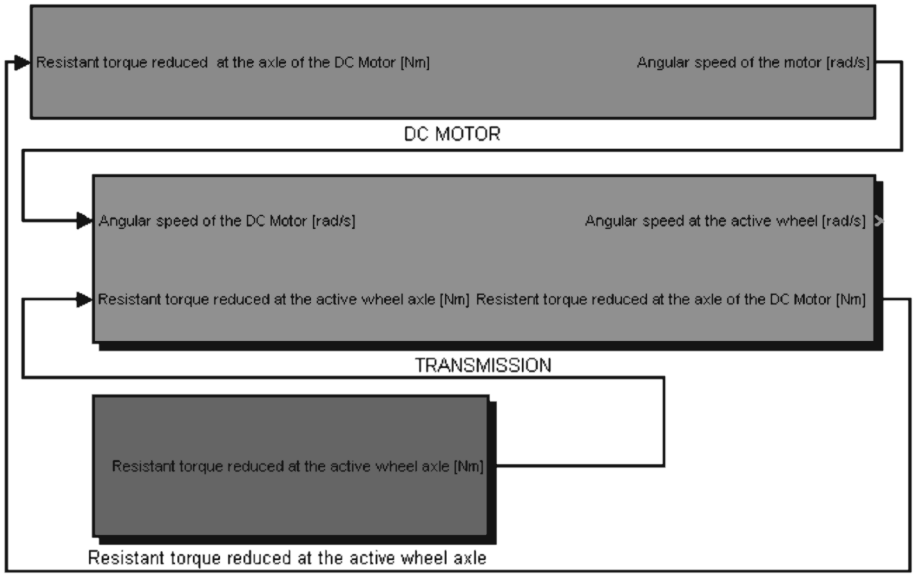

Fig. 11. Matlab/Simulink model of the robotic system

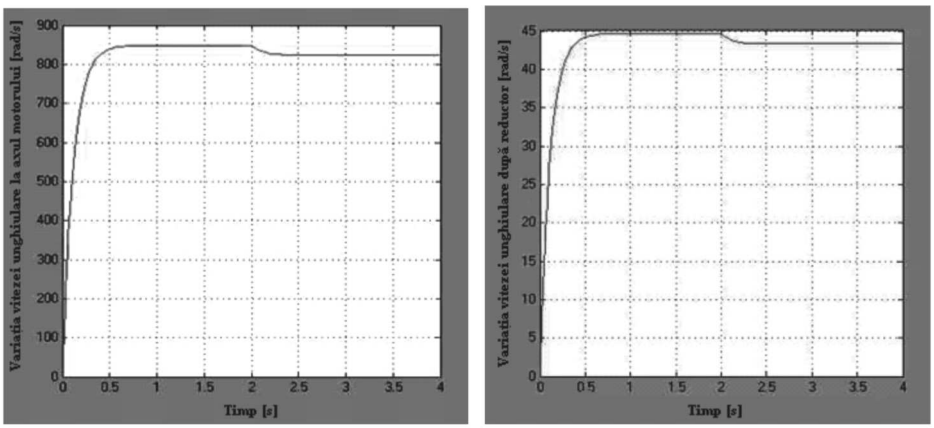

a) b)

www.czasopisma.pan.pl PAN POLSKA AKADEMIA NAUK www.journals.pan.pl

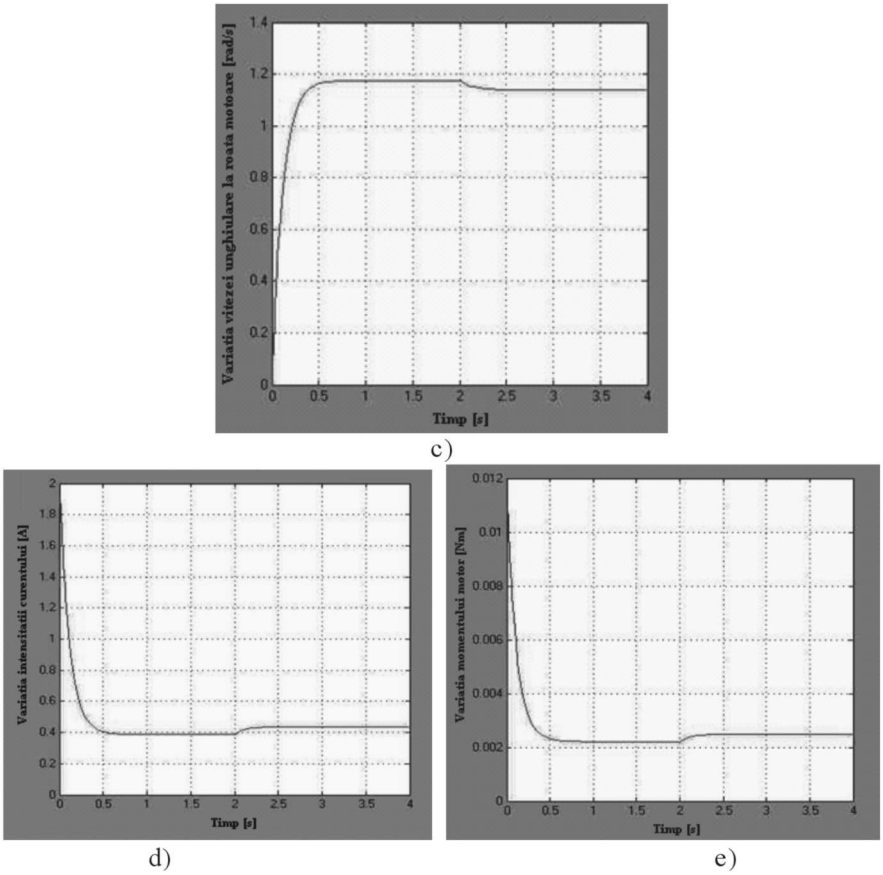

Fig. 12. Angular speed variation at the axle of the DC motor a), at the axle of the reducer ($i_{reducer}$ = 19) b), at the active wheel ($i_{transmission}$ = 38) c), the current intensity d) and the motor torque e), for the case that we apply the exteriour load as a step signal, at 2 seconds after the start of the simulation

For the DC motor model, several types of motors available on the market were tested. These motors had the required design, but some of the characteristics, such as torque and power consumption, were different. After the simulation, the best results were obtained by using the *IG 22* series motor, which had the following output data: $b = 2.6 \cdot 10^{-6} Nm/ rad/s$; $K = 5.7 \cdot 10^{-3} Nm/A$; $R = 3\ \Omega$; $L = 6\ mH$ and $I^r = I = 1.5 \cdot 10^{-6} kgm^2$. Using a 6V voltage, the number of revolutions per minute of the motor axle was $n = 8100\ rpm$, the angular speed was $\omega = 848.23\ rad/s$, the current intensity $I = 75\ mA$, the power $P = 1.5\ W$ and the torque in the axle of the motor was $M = 1.768 \cdot 10^{-3} Nm$. For the active wheel the number of revolutions per minute was $n = 11.219\ rpm$, the angular speed $\omega = 1.175\ rad/s$ and the torque of the active wheel was $M = 1.277\ Nm$. The condition that requires

www.czasopisma.pan.pl PAN POLSKA AKADEMIA NAUK www.journals.pan.pl

the torque of the motor to be higher than the reduced torque at the axle of the motor is done.

3. The developed prototype of modular robotic system

The prototype is able to inspect pipes with the interior diameter ranging between 135 and 180 mm. It weights 1980 g and has a length of 856 mm. The prototype is presented in Figure 13.

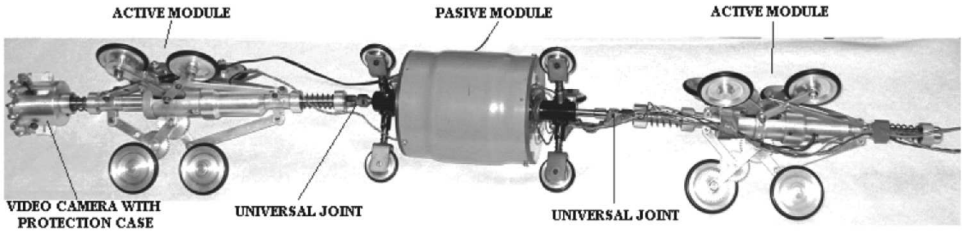

Fig. 13. Developed prototype

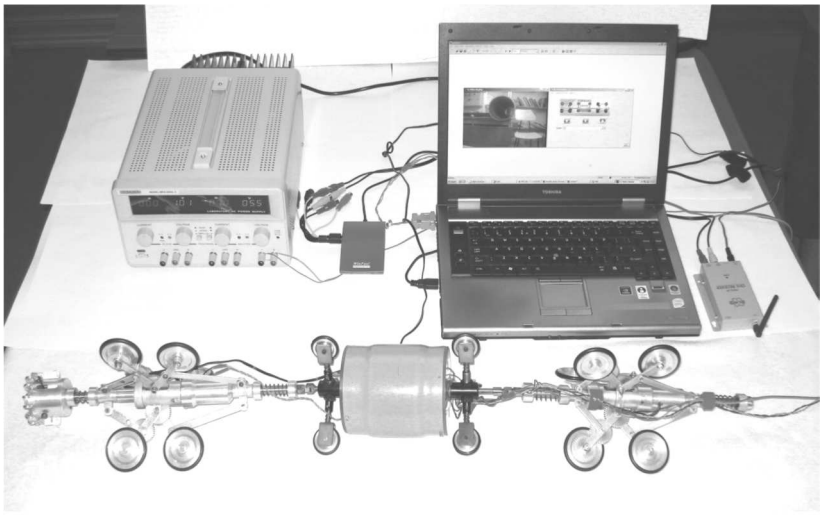

Fig. 14. Image from the test of the prototype

The force exerted on the inner pipe walls for all prototypes is generated with the help of a compression spring. The springs placed on the central axis assure the repositioning of the structure in the event of pipe diameter variation. For the control of the speed of the system, the PWM method was used, and data from the user were transmitted from a PC user interface specially developed in Borland DELPHI.

www.czasopisma.pan.pl PAN POLSKA AKADEMIA NAUK www.journals.pan.pl

The speed of the prototype in horizontal surface pipe segments, at 6 V supply voltage for the actuators, was 150 mm/s, and the maximum distance in which the tethered robot was functioning was 100 m. The images from the wireless camera were recorded in real time from a distance of maximum 50 m, enabling the user to gather data about the existence of internal fatigue or obstacles.

ACKNOWLEDGEMENTS

With the support of CNCSIS (National Council of Scientific Research in Higher Education from Romania); through PNII – IDEI Project, ID_1056: Modeling, simulation and development of robotic system families used for inspection and exploration.

Manuscript received by Editorial Board, December 24, 2010;
final version, February 07, 2011.

REFERENCES

[1] Choi H.R., Ryew S.M.: Robotic system with active steering capability for internal inspection of urban gas pipelines, Mechatronics, Vol. 12, pp. 713-736, 2002.
[2] Jun C., Deng Z., Jiang S.: Study of Locomotion Control Characteristics for Six Wheels Driven In-Pipe Robot, Proceedings of the 2004 IEEE International Conference on Robotics and Biomimetics, Shenyang, China, 2004.
[3] Roh S.G., Choi H.R.: Differential-drive in-pipe robot for moving inside urban gas pipelines, IEEE Transactions Robotics, Vol. 21, No. 1, pp. 1-17, 2005.
[4] Tătar M.O, Stan S., Mândru D.: The modular robotic systems, PAMM Volume 8, Issue 1, pp. 10311-10312, WILEY-VCH Verlag GmbH & Co. KGaA, Weinheim (Special Issue: 79th Annual Meeting of the International Association of Applied Mathematics and Mechanics (GAMM), Bremen 2008).
[5] Tătar M.O., Aluţei A., Mândru D.: Driving module for modular robotic system, in vol. Machine Design 2009, Ed. S. Kuzmanovic, University of Novi Sad, 2009, pp. 147-150.
[6] Tătar M.O., Aluţei A., Mândru D., Lungu I.: Minirobots with Adaptable Structure – Chapter 21 in DAAAM International Scientific Book 2009, pp. 187-196, B. Katalinic (Ed.), Published by DAAAM International, ISBN 978-3- 01509-69-8, ISSN 1726-9687,Vienna, Austria, DOI: 10.2507/daaam.scibook.2009.21
[7] Tătar M. O., Aluţei A., Mândru D.: In-pipe Modular Robotic Systems for Inspection and Exploration, Solid State Phenomena Vol. 164 (2010) pp 425-430, Trans Tech Publications, Switzerland doi:10.4028/www.scientific.net/SSP.164.425

Opracowanie modularnego systemu inspekcyjnego

Streszczenie

Celem artykułu jest prezentacja systemu robota do prac we wnętrzu rur, który może nawigować w niedostępnych rurociągach przemysłowych celem sprawdzania ich stanu, lokalizacji przecieków i czyszczenia systemów wentylacyjnych. Zaprezentowano aspekty związane z opracowaniem lekkiego, wydajnego energetycznie modularnego systemu robota. Artykuł rozpoczyna się krótkim wprowadzeniem. W rozdziale pierwszym omówiono modularne systemy inspekcyjne, w dalszej części przedstawiono aspekty projektowania, a w zakończeniu podano wyniki testów opracowanego systemu robota.